β- and γ-decay spectroscopy of ^{197,198}Os

Y. Hirayama,[1,*] Y. X. Watanabe,[1] M. Mukai,[1,2,3] M. Ahmed,[1,2] S. C. Jeong,[1,4] Y. Kakiguchi,[1] S. Kimura,[1,2,3] M. Oyaizu,[1]
J. H. Park,[4] P. Schury,[1] M. Wada,[1,3] H. Watanabe,[1,3,5] and H. Miyatake[1]

[1]*Wako Nuclear Science Center (WNSC), Institute of Particle and Nuclear Studies (IPNS),*
High Energy Accelerator Research Organization (KEK), Wako, Saitama 351-0198, Japan
[2]*University of Tsukuba, Tsukuba, Ibaraki 305-0006, Japan*
[3]*Nishina Center for Accelerator-Based Science, RIKEN, Wako, Saitama 351-0198, Japan*
[4]*Rare Isotope Science Project, Institute for Basic Science (IBS), Daejeon 305-811, Republic of Korea*
[5]*IRCNPC, School of Physics and Nuclear Energy Engineering, Beihang University, Beijing 100191, China*

We performed β and γ spectroscopy of ^{197g,198g}Os and ^{198g}Ir, which were produced by multinucleon transfer reactions at the KEK Isotope Separation System (KISS). KISS was designed for the study of nuclear spectroscopy in the vicinity of $N = 126$ for astrophysical interests. The β-decay half-life of ^{197g}Os was revised to 91(8) s, while the half-life of ^{198g}Os was measured for the first time and found to be 125(28) s. The β-decay schemes of ^{198g}Ir and ^{198g}Os were partially established from this spectroscopic study. Based on presently suggested $I^\pi = (3/2$ or $5/2)^-$ and $(0$ or $1)^-$ for ^{197g}Os and ^{198g}Ir, respectively, the first-forbidden transitions of $\nu(3p_{3/2})$ or $\nu(2f_{5/2}) \rightarrow \pi(2d_{3/2})$ are suggested to be dominant.

I. INTRODUCTION

The study of β-decay half-lives of waiting-point nuclei with $N = 126$ is crucial in understanding the explosive astrophysical environment associated with the third peak in the observed solar abundance pattern, which is produced by a rapid neutron capture process (r process) [1,2]. Because half-lives govern the time scale of the explosive process and they determine the abundance peak structure around $A = 195$ such as its peak height, position, and width. However, half-life measurements of the waiting-point nuclei are impracticable because producing the nuclei is difficult. Therefore, accurate theoretical predictions for the half-lives are required in investigations into astrophysical environments.

To improve and verify the theoretical models [3–5] that predict not only half-lives but also nuclear masses, it is essential to measure the half-lives [6–8] and derive the β-decay schemes including spin-parity I^π values of as many nuclei in the vicinity of $N = 126$ as possible to understand the competition between the allowed Gamow-Teller (GT) and first-forbidden (FF) β-decay transitions. Indeed, this competition makes it difficult to predict the nuclear properties in this region. For example, the proton orbit of neutron-rich nuclei around $N = 126$ is $\pi(1h_{11/2})$, and hence the GT transition from $\nu(1h_{9/2})$ to $\pi(1h_{11/2})$ and the FF transition from $\nu(1i_{13/2})$ to $\pi(1h_{11/2})$ compete. In the region $N \leqslant 126$, the FF transitions of $\nu(3p_{1/2})$ or $\nu(3p_{3/2}) \rightarrow \pi(3s_{1/2})$ and $\nu(2f_{5/2})$ or $\nu(3p_{3/2}) \rightarrow \pi(2d_{3/2})$ are expected to dominate. β and γ spectroscopy including the assignment of I^π, which play an important role in studying β-decay transitions, are used to eliminate uncertainty

and improve predictions of nuclear properties by ensuring the FF transition is accounted for correctly.

For the ground state ^{197g}Os, one β-decay spectroscopy study [9] was previously reported. However, the particle identification of ^{197g}Os produced in the $^{nat.}$Pt + n (14 MeV) reactions were not performed and there seems to be ambiguity concerning the reported half-life and β-delayed γ rays. For ^{198g}Os, there have been no previously reported β-decay spectroscopy studies and its half-life is unknown. In this paper, we report the experimental results from the β- and γ-decay spectroscopy of ^{197g,198g}Os. One of the advantages of the present study is the firm selection and identification of ^{197g,198g}Os using the KEK isotope separation system (KISS) [10–12], which can extract an isotope of interest with a small amount of contamination for precise nuclear spectroscopy. Therefore, we can deduce the half-lives from the traditional decay-curve measurements with much simpler analyses (and without ambiguity) than the evaluations of half-lives measured at in-flight facilities [6–8].

II. EXPERIMENT

The experiment was performed by using KISS [10–12], an argon-gas-cell-based laser ion source combined with an on-line isotope separator, installed at the RIKEN Nishina center. The primary beam ^{136}Xe (10.75 MeV/A, 50 pnA), accelerated by the RIKEN Ring Cyclotron, was incident on an enriched ^{198}Pt (purity 91.63%) target with a thickness of 12.5 mg/cm^2. The unstable nuclei ^{196g,197g,198g}Os ($Z = 76$ and $N = 120$, 121, 122) and ^{198g}Ir ($Z = 77$ and $N = 121$), among others, were produced by multinucleon transfer (MNT) reactions [13]. The MNT reaction products were accumulated, thermalized, and neutralized in a doughnut-shaped argon-filled gas cell [12] pressurized at 88 kPa. The gas cell was optimally designed for

*yoshikazu.hirayama@kek.jp

the efficient gas-flow transportation of neutral isotopes toward the exit.

A two-color two-step resonant laser ionization technique [10,14,15] was applied to re-ionize the isotopes in the gas cell. This technique allows nuclei with an atomic number Z of interest to be selected. In the experiment, a tunable dye laser (Radiant Dyes Laser; NarrowScan) pumped by a XeCl:excimer laser ($\nu = 308$ nm, Lambda Physik LPX240i) was used for the first step excitation ($\nu_1 = 247.758$ nm for osmium [14] and 247.582 nm for iridium [16]) with a laser power of 100 μJ/pulse. Here, the resonance widths of these elements were observed to be approximately 0.010 nm at full width at half-maximum (FWHM). Therefore, by adjusting the ν_1 to osmium or iridium isotopes and accounting for the pressure and isotope shifts of ν_1 [14,16], the element of interest is selected by laser resonance ionization technique, and the selected isotope is extracted from the KISS gas cell. Another XeCl excimer laser of $\nu_2 = 308$ nm with a laser power of 12 mJ/pulse was used for the ionization transition to the continuum above the ionization potential (IP).

The laser-produced, singly charged ($q = 1$) radioactive ions were accelerated with an energy of 20 kV, and the magnetic rigidity of a dipole magnet selects ions of the desired mass-to-charge ratio (A/q). Finally, the isotope of interest was transported to the detector station located in an adjacent experimental hall with the probability around 10^{-3}. Simultaneously, reaction products with the same A/q, which may have survived as a singly charged ions in the gas cell, would be transported to the detector station with a probability around $\leqslant 10^{-4}$. The probability was deduced as a ratio of the measured implantation rate of the contaminant to the estimated production rate. Here, the production rates at the target were evaluated from the GRAZING predictions [17,18] normalized by using the measured production cross sections with an energy of 8 MeV/A at GANIL [13]. These are potential contaminants and make background events for the spectroscopy.

A tape transport device in the detector station was used to avoid radioactivity from the decay chains of the separated nuclides under the pulsed beam operation of KISS. An aluminized Mylar tape (12 μm in thickness) was moved at the end of each measurement cycle, which depends on the half-lives of the ground and isomeric states, to remove unwanted radioactivity from the detection area.

The radioactive isotope was implanted in the tape, which was surrounded by a high-efficiency and low-background multisegmented (32 counters make 16 pairs of telescope) proportional gas counter (MSPGC) for β-ray detection [19]. This counter is sensitive to not only β rays but also characteristic x rays and internal conversion electrons. These events are identified by analyzing the multiplicity (M) of the gas-counter hit patterns [19]. Therefore, it is possible to identify γ rays of internal transitions emitted from an isomeric state by detecting the following characteristic x rays and/or internal conversion electrons, which were mainly $M = 1$ (only one counter of the MSPGC is fired) and also $M = 2$ events (only one telescope of the MSPGC is fired). The absolute detection efficiency of the 16 telescope pairs in the MSPGC is as high as about 50% for β rays ($M = 2$ events) emitted from the osmium and iridium isotopes because of a lower energy threshold
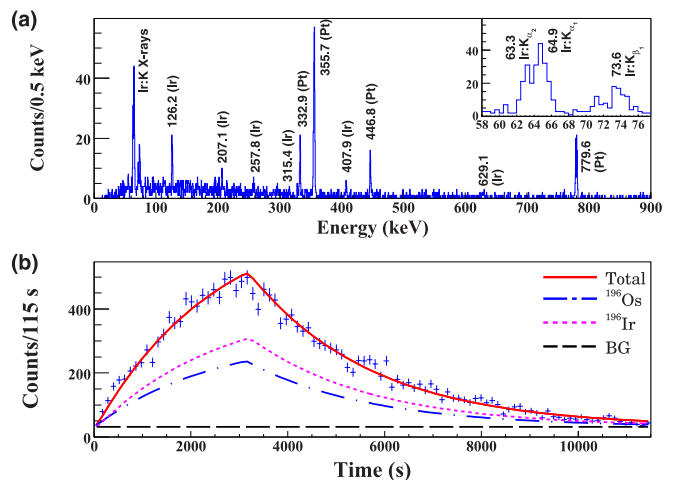
FIG. 1. β-decay spectroscopy was performed under the experimental particle-selection condition of osmium ($Z = 76$) selection by laser resonance ionization and $A/q = 196$ selection. (a) Measured γ-ray energy spectrum in coincidence with the MSPGC ($M = 2$). The inset in (a) is an enlarged view of the low-energy region. The reported γ rays [20] with intensities of more than 1% per β decay were identified in the present experiment. Here, the γ-ray peaks labeled as Ir and Os indicate that those were, respectively, emitted from ^{196}Ir and ^{196}Pt populated by the β decays of the parent nucleus ^{196g}Os and daughter nucleus ^{196g}Ir. (b) Half-life measurement by detecting β rays using the MSPGC ($M = 2$). Here, the time sequence of the KISS beam is $T_{on}/T_{off} = 3141/8376$ s. Solid line (red) is the best-fit curve, which consists of the β-detection growth and decay curve $f(t)$ [dash-dotted (blue) line] associated with ^{196g}Os ($T_{1/2}$ and the implantation rate are free parameters), the curve $g(t)$ associated with the daughter nucleus ^{196g}Ir [dotted (purple) line, fixed $T_{1/2} = 52$ s [21] and amplitude was restricted by the implantation rate of ^{196g}Os], and the constant background I_{BG} [long-dashed (black) line].

of around 100 keV than that of typical plastic-scintillator β telescopes.

Four super clover Ge detectors were installed to detect β-delayed γ rays and γ rays from the internal transition of isomeric states. The absolute detection efficiency was calibrated using γ rays from ^{152}Eu and ^{133}Ba, and the efficiency for γ rays with an energy of 400 keV was measured at about 14%.

III. RESULTS

A. β-decay spectroscopy of ^{196g}Os

To confirm the firm extraction of laser-ionized osmium isotopes from KISS by performing the β-γ spectroscopy of ^{196g}Os ($T_{1/2} = 34.9 \pm 0.2$ min) [20], the mass-separator parameters and the excitation laser wavelength ν_1 were adjusted for the selections of $A/q = 196$ and ^{196g}Os, respectively. Figure 1(a) shows the measured γ-ray energy spectrum in coincidence with the MSPGC ($M = 2$). We confirmed that the γ rays with intensities of more than 1% per β decay were consistent with the reported γ rays [20]. Moreover, it was confirmed that there was no contaminant in the present measurement for ^{196g}Os. We also measured the half-life of ^{196g}Os, as shown in Fig. 1(b), and

found a half-life $T_{1/2} = 35.3 \pm 1.4 \, \text{min}$ (reduced $\chi^2 = 0.90$) consistent with that previously reported value [20]. Thus, we firmly extracted ^{196g}Os from KISS and identified ^{196g}Os from these measurements.

The half-life and implantation rate $I_0 = 7.1(7)$ particles per second (pps) of ^{196g}Os were deduced from the analysis of a measured time spectrum such as that shown in Fig. 1(b) by using the following equations:

$$\frac{dN_p(t)}{dt} = \begin{cases} I_0 - \lambda_p N_p(t) & (0 \leqslant t \leqslant T_{\text{on}}), \\ -\lambda_p N_p(t) & (T_{\text{on}} \leqslant t \leqslant T_{\text{on}} + T_{\text{off}}), \end{cases} \quad (1)$$

$$\frac{dN_d(t)}{dt} = \lambda_p N_p(t) - \lambda_d N_d(t), \quad (2)$$

where $N_i(t)$ and $\lambda_i(= \ln 2/T_{1/2})$ ($i = p$ or d) are the number of implantation of a given nucleus as a function of the measurement time t and its decay constant, respectively. The subscripts $i = p$ and d refer to the parent and daughter nuclei, respectively. In the present case, p and d refer to ^{196g}Os and ^{196g}Ir, respectively. T_{on} and T_{off} are KISS beam ON and OFF periods, respectively. The functions $f(t)$ and $g(t)$, respectively, represent the number of β rays from the parent and daughter nuclei detected by the MSPGC. These equations were deduced from Eqs. (1) and (2), respectively, as follows:

$$f(t) = C_N \epsilon_{\beta,p} \lambda_p N_p(t), \quad (3)$$

$$g(t) = C_N \epsilon_{\beta,d} \lambda_d N_d(t). \quad (4)$$

C_N is the number of KISS beam ON/OFF cycles in the measurement. Using GEANT4, the efficiency for detection of β rays from the parent ($\epsilon_{\beta,p}$) and daughter ($\epsilon_{\beta,d}$) were evaluated [19]. The functions $f(t)$, $g(t)$ and the constant background I_{BG} were used to fit the time spectrum in Fig. 1(b). I_0, λ_p, and I_{BG} were always free parameters in the analyses to deduce half-lives and implantation rates. Previously reported values [21] of the decay daughter's half-life were used to fix λ_d. The functions $f(t)$ and $g(t)$ were used to evaluate the half-lives and implantation rates of ^{197g,198g}Os and ^{198g}Ir in the following subsections. The functions $f(t)$ and $g(t)$ for contaminant nuclei were also taken into account in the fitting analysis, and all the parameters for contaminant nuclei were fixed to the reported half-lives [21] and the independently evaluated implantation rates.

B. β-decay spectroscopy of ^{197}Os

To perform the β-γ spectroscopy of ^{197g}Os [$T_{1/2} = 2.8(6) \, \text{min}$] [21], the mass-separator parameters and the excitation laser wavelength ν_1 were adjusted for the selections of $A/q = 197$ and ^{197g}Os, respectively. Figure 2(a) shows the γ-ray energy spectrum in coincidence with the MSPGC ($M = 2$) for the spectroscopy of the laser-ionized ^{197g}Os$^+$ decaying to ^{197g}Ir [$T_{1/2} = 5.8(5) \, \text{min}$] $\rightarrow$ ^{197g}Pt [$T_{1/2} = 19.892(2) \, \text{h}$] $\rightarrow$ ^{197g}Au (stable). To mitigate contamination of β-delayed γ-rays emitted from the daughter nucleus ^{197}Ir, the measurement in Fig. 2(a) was performed with a time sequence of KISS beam ON/OFF: $T_{\text{on}}/T_{\text{off}} = 180/1 \, \text{s}$. The dose ratio of β decays between ^{197g}Os and ^{197g}Ir was about 10, accounting for their half-lives and the time sequence. Therefore, β-delayed
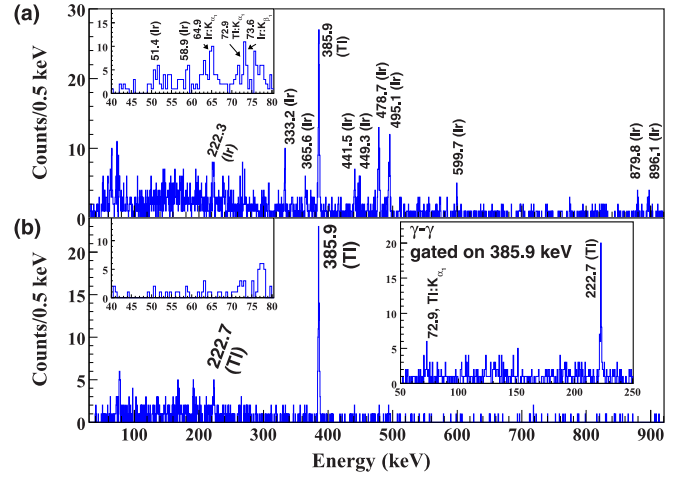
FIG. 2. Measured γ-ray energy spectra in coincidence with the MSPGC ($M = 2$). The experimental particle-selection condition was osmium ($Z = 76$) selection by laser resonance ionization and $A/q = 197$ selection. Here, the γ-ray peaks labeled as Ir and Tl indicate that those were, respectively, emitted from the daughter nuclei of ^{197}Ir populated by the β decay of ^{197g}Os and the internal decay of the contaminant nucleus ^{197m}Tl [$T_{1/2} = 0.54(1) \, \text{s}$]. (a) γ-ray energy spectrum measured in the time sequence of $T_{\text{on}}/T_{\text{off}} = 180/1 \, \text{s}$. The inset is an enlarged view of low-energy region of 60–80 keV. The observed intense 385.9(1) keV γ-ray peak stemmed from the contaminant of an isomeric state ^{197m}Tl. Other γ rays were emitted from ^{197}Ir excited states. (b) γ-ray energy spectrum measured in the time sequence of $T_{\text{on}}/T_{\text{off}} = 6/3 \, \text{s}$ for the particle identification of the isomeric state ^{197m}Tl. The left and right insets are enlarged views of low-energy region of 60–80 keV and γ-γ coincidence spectrum (without β-ray gate) gated on the γ ray with $E_\gamma = 385.9 \, \text{keV}$, respectively.

γ rays emitted from ^{197g}Os were predominantly measured. Characteristic x rays corresponding to iridium and many γ-ray peaks were observed and summarized in Table I. The existence of characteristic x rays indicated that the ^{197g}Os extracted from KISS were transported to the detector station and that internal conversion electrons were emitted from low-energy internal transitions of ^{197}Ir states, which were populated by the β decays of ^{197g}Os.

In the γ-ray energy spectra coincident with the MSPGC as shown in Fig. 2, internal-transition γ rays from an isomeric state and characteristic x rays were measured by the Ge detectors in coincidence with the MSPGC, which detected conversion electrons associated with the cascade transitions. The characteristic x rays of thallium and the intense 385.9(1) keV γ-ray peak in Fig. 2(a) indicate the existence of a contamination by the long-lived isomeric state ^{197m}Tl [$Z = 81$, $N = 116$, $I^\pi = 9/2^-$, $E_{\text{ex}} = 608.2 \, \text{keV}$, and $T_{1/2} = 0.54(1) \, \text{s}$] [21], which internally decays via the cascade transitions of 222.45(5) keV and 385.8(3) keV as follows: ^{197m}Tl ($E_{\text{ex}} = 608.2 \, \text{keV}$, $I^\pi = 9/2^-$, E3 transition) $\rightarrow$ ^{197*}Tl ($E_{\text{ex}} = 385.8 \, \text{keV}$, $I^\pi = 3/2^+$, M1 transition) $\rightarrow$ ^{197g}Tl ($I^\pi = 1/2^+$, $T_{1/2} = 2.84 \, \text{h}$).

To clarify the contamination of the isomeric state and its influence on the evaluation of ^{197g}Os half-life, β-γ spectroscopy and half-life measurement were performed with the

TABLE I. Measured half-lives and γ-ray intensities per β decay emitted from the selectively-laser-ionized ^{197g}Os. Here, the intensities are without corrections for internal conversion. The excited states with I^π reported in Ref. [28] are listed by accounting for the reported level energies with the uncertainties.

Nuclide: $T_{1/2}$ (s)	Present work				Reported state [28]	
	E_γ (keV)	I_γ (%)/β decay	$T_{1/2}$ (s) gated on E_γ	log(ft)	E_x (MeV)	I^π
^{197g}Os: 91(8)	0.0	$\geqslant$66(3)	–	$\leqslant$5.93(4)	0	$3/2^+$
	51.4(2)	1.7(8)	166(61)	7.5(2)	52(5)	$1/2^+$
	58.9(2)	1.1(6)	112(52)			
	222.3(2)	1.2(9)	131(31)	7.5(3)	224(5)	–
	333.2(2)	3.1(8)	121(54)			
	365.6(3)	2.0(6)	58(37)			
	441.5(2)	2.8(8)	68(44)			
	449.3(3)	1.8(6)	167(2098)			
	478.7(1)	7.4(14)	116(23)			
	495.1(2)	5.5(12)	109(26)	6.7(1)	495(5)	–
	599.7(3)	1.7(6)	27(21)	7.1(2)	606(5)	$5/2^+$
	879.8(4)	1.8(7)	68(44)	6.9(2)	885(5)	–
	896.1(3)	2.6(8)	70(59)			

time sequence of $T_{on}/T_{off} = 6/3$ s. In the energy spectra in Fig. 2(b), most of the γ rays observed in Fig. 2(a) disappeared, and an intense γ-ray peak at $E_\gamma = 385.9(1)$ keV is evident. This strongly supports the 385.9 keV γ ray having been emitted from ^{197m}Tl with a known short half-life of $T_{1/2} = 0.54(1)$ s as compared with $T_{1/2} = 2.8(6)$ min of ^{197g}Os, while most γ rays observed in Fig. 2(a) were emitted from ^{197g}Os as the β-delayed γ rays. The left inset of in Fig. 2(b) shows the enlarged view of the low-energy spectrum spanning from 60 keV to 80 keV, while the right inset shows the γ-γ coincidence spectrum gated on 385.9 keV γ ray but not β-ray gated. In the γ-γ coincidence spectrum, a γ ray with $E_\gamma = 222.7(2)$ keV and the thallium characteristic x ray were observed. The energies of 222.7(2) keV and 385.9(1) keV γ rays were in good agreement with previously reported γ-ray emissions from ^{197m}Tl [21].

Figure 3(a) shows the time spectrum measured in coincidence with the 385.9-keV γ ray. The half-life of the isomeric state was evaluated to be 0.56(10) s with a reduced $\chi^2 = 0.97$ from Fig. 3(a), which was consistent with the reported 0.54(1) s half-life of ^{197m}Tl.

The implantation rate I_0 of ^{197m}Tl and the conversion coefficient α for the 222.7(2) and 385.9(1)-keV γ rays were evaluated from the measured event numbers of $N_{\beta-\gamma i}$ and $N_{\gamma i}$ in β(conversion electron)-γ and γ-single energy spectra, respectively, with the time sequence of $T_{on}/T_{off} = 6/3$ s. The subscripts $i = 1$ and 2 refer to the γ rays with $E_\gamma = 222.7$ keV and 385.9 keV, respectively. In the analysis, total internal-decay dose N_m of ^{197m}Tl in the time sequence was applied for the evaluations, and it was expressed by using the decay constant λ_p and Eq. (1) (including the implantation rate I_0) as follows:

$$N_m = C_N \int_0^{T_{on}+T_{off}} \lambda_p N_p(t)dt. \quad (5)$$

Then, I_0 and α were evaluated by using N_m and the following equations:

$$N_m \epsilon_{e2} w_{e2} \epsilon_{\gamma 1} w_{\gamma 1} = N_{\beta-\gamma 1},$$

$$N_m \epsilon_{e1} w_{e1} \epsilon_{\gamma 2} w_{\gamma 2} = N_{\beta-\gamma 2},$$

$$N_m \epsilon_{\gamma 1} w_{\gamma 1} = N_{\gamma 1},$$

$$N_m \epsilon_{\gamma 2} w_{\gamma 2} = N_{\gamma 2},$$

$$w_{ei} + w_{\gamma i} = 1 \quad (i = 1, 2),$$

where $\epsilon_{\gamma i}$, $\epsilon_{e i}$, $w_{\gamma i}$, and $w_{e i}$ are, respectively, the γ-ray detection efficiency of the Ge detectors, conversion-electron detection efficiency of the MSPGC, γ-ray emission probability, and conversion-electron emission probability. The detection efficiency $\epsilon_{\gamma i}$ was measured using ^{152}Eu and ^{133}Ba sources, and the detection efficiency $\epsilon_{e i}$ was evaluated using GEANT4 simulations [19]. The implantation rate I_0 of ^{197m}Tl was evaluated to be 0.8(1) pps by solving the equations. The conversion coefficient $\alpha_1 = 2.2(11)$ and $\alpha_2 = 0.14(9)$ were deduced by using the ratio $w_{ei}/w_{\gamma i}$ ($i = 1$, 2) based on the measurements. These values were found to be in good agreement with the previously measured $\alpha_{222.7\,keV} = 2.28$ and $\alpha_{385.9\,keV} = 0.094$ [22] for $E3$ and $M1$ transitions from ^{197m}Tl, respectively. From these measurements and analyses, we firmly identified the contaminant nucleus ^{197m}Tl with the implantation rate 0.8(1) pps.

In the case of ^{199m}Pt isomer produced by the MNT reactions, the implantation rate of ^{199m}Pt was measured to be about half of that of ^{199g}Pt [15]. Accounting for the experimental isomeric ratio [15] of unstable nuclei produced by the MNT reactions, we expected that ^{197g}Tl was likely present with a rate of ~1.6 pps, however its long half-life ($T_{1/2} = 2.84$ h) precluded its observation. The intensities of the contamination indicated that ^{197m,g}Tl$^+$ were extracted from the KISS gas cell with a probability of ~10^{-4}.

Finally, we performed half-life measurements of ^{197g}Os with the time sequence of $T_{on}/T_{off} = 252/672$ s. Figure 3(b) shows β-detection growth and decay curves associated with ^{197g}Os using $M = 2$ events in the MSPGC. The half-life of ^{197g}Os was evaluated using Eqs. (3) and (4) for the β decay of the parent nucleus ^{197g}Os and the daughter nucleus ^{197g}Ir, respectively. Both functions expressed by Eqs. (3) and (4) for the internal decay of ^{197m}Tl and the β decay of ^{197g}Tl (both

subsequent to internal decay of ^{197m}Tl and directly implanted) were used simultaneously in the time spectrum analysis. Due to its very long half-life, the effect of β decay from ^{197g}Hg ($T_{1/2} = 2.7$ d), the daughter nucleus of ^{197g}Tl, was neglected. The evaluated implantation rate of ^{197m}Tl (0.8 pps) and the estimated implantation rate of ^{197g}Tl (1.6 pps) were used in the analysis. The resultant half-life measured for ^{197g}Os, $T_{1/2} = 91(8)$ s (reduced $\chi^2 = 1.22$), deviates by nearly 2-σ from the previously accepted value of 168(36) s. Because the half-life ^{197g}Tl was much longer than that of ^{197g}Os, functions related to ^{197g}Tl did not affect the evaluation of half-life of ^{197g}Os significantly. The implantation rate of ^{197g}Os was evaluated to be 2.1(2) pps from the fit in Fig. 3(b).

For ^{197g}Os, 12 γ rays were identified as β-delayed γ ray by independently evaluating the half-life from each β-gated γ-ray peak, as listed in Table I. The half-life gating on the intense γ rays with $E_\gamma = 478.7$ and 495.1 keV was 101(18) s, as shown in Fig. 3(c), which is consistent with 91(8) s half-life we determined for ^{197g}Os. From these half-life measurements, we find that while the 222.7(2) keV γ rays is from the internal decay of ^{197m}Tl, there is a 222.3(2) keV β-delayed γ ray with
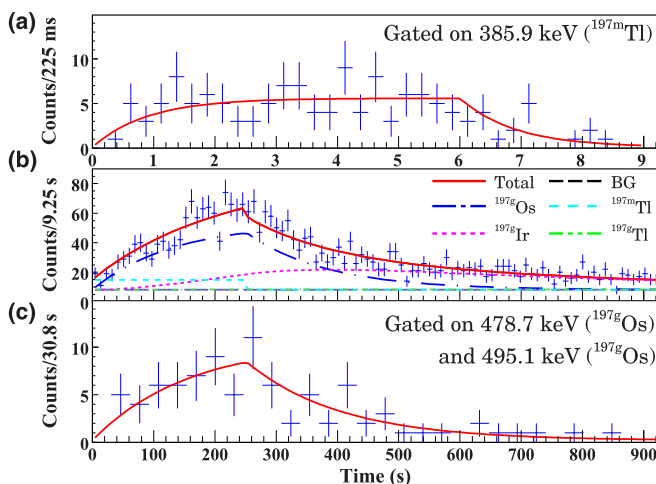
FIG. 3. (a) time spectrum obtained by gating on the 385.9-keV γ ray emitted from the contaminant nucleus ^{197m}Tl, which was measured in the time sequence of $T_{on}/T_{off} = 6/3$ s. Here, $T_{1/2}$ and amplitude are free parameters. (b) measured time spectrum of the β ray detected by the MSPGC ($M = 2$) in the time sequence of $T_{on}/T_{off} = 252/672$ s for the case of ^{197g}Os. Solid line (red) is the best-fit curve, which consists of the constant background [long-dashed (black) line, free parameter] and four β-detection growth and decay curves as follows: dash-dotted (blue) line for ^{197g}Os ($T_{1/2}$ and implantation rate were free parameters), dotted (purple) line for the daughter nucleus ^{197g}Ir (fixed $T_{1/2} = 5.8$ min [21] and amplitude was restricted by the implantation rates of ^{197g}Os), dashed line (cyan) for ^{197m}Tl ($T_{1/2} = 0.54$ s and the implantation rate were fixed), double-dotted-dashed line (green) for ^{197g}Tl ($T_{1/2} = 2.84$ h and the implantation rate were fixed). The line of ^{197g}Tl included two components stemmed from the ^{197g}Tl populated by the internal decay of ^{197m}Tl and the directly-implanted ^{197g}Tl. (c) time spectrum obtained by gating on the 478.7 and 495.1-keV γ rays emitted from ^{197g}Os as the β-delayed γ ray, which were measured in the time sequence of $T_{on}/T_{off} = 252/672$ s. Here, $T_{1/2}$ and amplitude are free parameters.
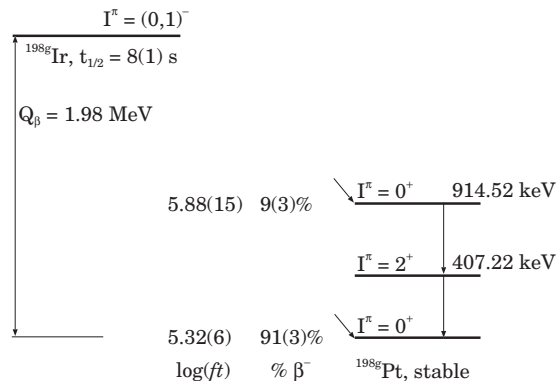
FIG. 4. Decay scheme of ^{198g}Ir. The β-decay intensities and the related $\log(ft)$ values were newly measured. Half-lives, spin-parity values, Q_β and γ-transition energies were the previously reported values [21].

an intensity of 1.2(9)% per β decay of ^{197g}Os. The other γ rays listed in Table I show half-lives consistent with 91(8) s. Therefore, these γ rays were concluded to be β-delayed γ rays of ^{197g}Os. Even though there might be some possibilities of the contamination of other isobars (other elements) with $A/q = 197$, we did not identify any γ rays from these in the present measurements.

In the present measurement, we did not observe the previously reported intense γ rays with energies of $E_\gamma = 342.1$ and 403.6 keV [9], which had been used to deduce the half-life of ^{197g}Os. The origin of these γ rays, recently measured in a previous experiment [9], were considered to stem from an unreported ^{197g}Os β decay. However, the particle identification of ^{197g}Os produced in the $^{nat.}$Pt $+ n$ (14 MeV) reactions were not performed in that experiment. Therefore, the assignments of these γ rays may be mistaken because there was no firm selection and identification of ^{197g}Os in the previous measurement [9].

C. β-decay spectroscopy of ^{198}Ir

To perform the β-γ spectroscopy of ^{198g}Ir [$T_{1/2} = 8(1)$ s] [21] before the extraction of laser ionized ^{198}Os$^+$, the mass-separator parameters and the excitation laser wavelength ν_1 were adjusted for the selections of $A/q = 198$ and ^{198g}Ir, respectively. Figure 5(a) shows the γ-ray energy spectrum obtained in coincidence with the MSPGC ($M = 2$) for the spectroscopy of laser-ionized ^{198g}Ir$^+$ decaying to the stable nucleus ^{198g}Pt. The implantation rate of 3.0(4) pps was evaluated from the fit to the time spectrum measured by the MSPGC. Consistent with previous reports, we measured a half-life of 9.1(8) s and γ rays with energies E_γ of 407.22 keV and 507.3 keV [21], which were emitted from the decay of ^{198g}Ir $\rightarrow$ ^{198*}Pt ($E_{ex} = 914.52$ keV, $I^\pi = 0^+$) $\rightarrow$ ^{198*}Pt ($E_{ex} = 407.22$ keV, $I^\pi = 2^+$) $\rightarrow$ ^{198g}Pt ($I^\pi = 0^+$). The evaluated γ-ray intensity per β decay for both γ rays was 9(3)%. From this result, it was concluded that the β-transition branching ratios to the ground and excited states at $E_{ex} = 914.52$ keV were 91(3)% and 9(3)% with $\log(ft)$ values of 5.32(6) and 5.88(15), respectively, as shown in Fig. 4.
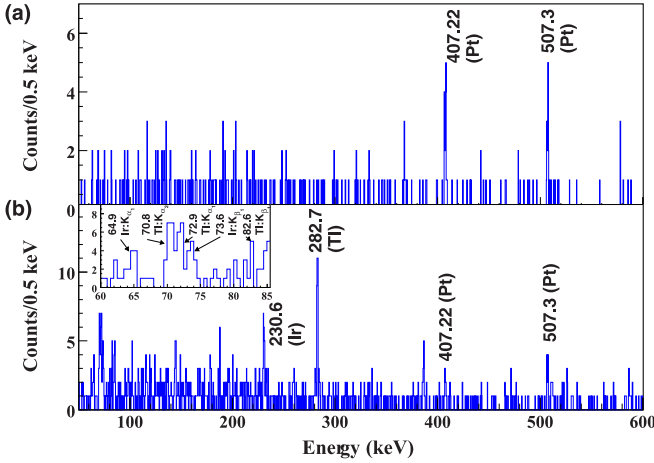
FIG. 5. Measured γ-ray energy spectra in coincidence with the MSPGC ($M = 2$). Here, the experimental particle-selection conditions were $A/q = 198$ selection, and (a) iridium ($Z = 77$) and (b) osmium ($Z = 76$) selections by laser resonance ionization. Here, the γ-ray peaks labeled as Ir, Pt, and Tl indicate that those were emitted from ^{198}Ir and ^{198}Pt, respectively, populated by the β decays of the parent nucleus ^{198g}Os and the daughter nucleus ^{198g}Ir, and the internal decay of the contaminant nucleus ^{198m}Tl. (a) β-delayed γ-ray energy spectrum of laser-ionized ^{198g}Ir$^+$ ($T_{1/2} = 8(1)$ s [21]). The time sequence in the measured was $T_{\text{on}}/T_{\text{off}} = 12/32$ s. (b) γ-ray energy spectrum of laser-ionized ^{198g}Os$^+$ and the contaminant nucleus ^{198m}Tl ($T_{1/2} = 1.87$ h [21]). The inset in (b) is an enlarged view of the low-energy region of 60–85 keV.

Any γ-ray peaks from other isotopes, as shown in Fig. 5(a), were not identified in the present measurement with the time sequence of $T_{\text{on}}/T_{\text{off}} = 12/32$ s. This indicates that there would be no contaminants with similar half-lives to that of ^{198g}Ir, and also that there might be some possibilities of contamination whose half-lives are much longer as compared to the present time sequence.

D. β-decay spectroscopy of ^{198}Os

To perform the β-γ spectroscopy of ^{198g}Os ($T_{1/2} =$ unknown) after that of ^{198g}Ir, only the excitation laser wavelength ν_1 was adjusted for the selection of ^{198g}Os [14]. Figure 5(b) shows the γ-ray energy spectrum in coincidence with the MSPGC ($M = 2$) for the spectroscopy of laser-ionized ^{198}Os$^+$, which decays to ^{198g}Ir $\rightarrow$ ^{198g}Pt. Several γ rays and characteristic x rays were observed; see summary in Table II. The γ rays with $E_\gamma = 407.22$ keV and 507.3 keV were found to be emitted after the β decay of the daughter nucleus ^{198g}Ir. This confirmed that β decay of the parent nucleus ^{198g}Os was measured. Half-life measurements by gating on β rays and γ rays were performed not only to deduce the half-life of ^{198g}Os but also to clarify the origins of the γ rays with $E_\gamma = 230.6(2)$ and 282.7(2) keV.

The measured γ-ray energy of 282.7(2) keV was consistent with the reported transition energy of 282.8(2) keV from the isomeric state of ^{198m}Tl ($Z = 81$, $N = 117$, $I^\pi = 7^+$, $E_{\text{ex}} = 543.6$ keV, and $T_{1/2} = 1.87(3)$ h [21]), which internally decays via the cascade transitions of 260.9(3) keV and 282.8(2) keV

TABLE II. Measured β-decay half-lives and γ-ray intensities per β decay for the selectively-laser-ionized ^{198g}Ir and ^{198g}Os. Here, the intensities are without corrections for internal conversion.

Nuclide: $T_{1/2}$ (s)	E_γ (keV)	I_γ (%)/β-decay	$T_{1/2}$ (s) gated on E_γ
^{198g}Ir: 9.1(8)	407.22	9(3)	7.5(26)
	507.3	9(3)	17(11)
^{198g}Os: 125(28)	64.9[a]	11(5)	66(68)
	73.6[a]	13(5)	336(163)
	230.6(2)	20(6)	108(36)
	407.22[b]	10(4)	106(60)
	507.3[b]	12(5)	72(42)

[a]Iridium K x rays.
[b]β-delayed γ ray of daughter nucleus ^{198g}Ir.

as follows: ^{198m}Tl ($E_{\text{ex}} = 543.6$ keV, $I^\pi = 7^+$, $M4$ transition, $\alpha = 34$) $\rightarrow$ ^{198*}Tl ($E_{\text{ex}} = 282.8$ keV, $I^\pi = 3^-$, $M1$ transition, $\alpha = 0.46$) $\rightarrow$ ^{198g}Tl [$I^\pi = 2^-$, $T_{1/2} = 5.3(5)$ h]. The 282.7 keV γ rays were measured in β(conversion electron)-γ energy spectrum as shown in Fig. 5(b), because the energy of the 260.9(3) keV transition ($M4$) with $\alpha = 34$ is highly converted to a conversion electron which fired the MSPGC and was identified as β-ray event. This was also because the 260.9(3) keV γ ray were not identified in Fig. 5(b).

Figure 6(a) shows the time spectrum measured in coincidence with the 282.7-keV γ ray. The evaluated half-life in Fig. 6(a) was $\geqslant 30$ min, which supports that the 282.7 keV γ ray originated from ^{198m}Tl in keeping with the earlier observation of ^{197m}Tl contamination. The implantation rate of the contaminant nucleus ^{198m}Tl was evaluated to be 1.0(2) pps by accounting for the measured 282.7-keV γ-ray yield in Fig. 5(b) (corrected by the detection efficiency of the MSPGC and Ge detectors), the reported conversion-coefficient $\alpha = 0.46$ [21], and the total internal-decay dose N_{m} [Eq. (5)] of ^{198m}Tl in the present time sequence. ^{198g}Tl nucleus is also expected to be a probable contaminant with an implantation rate of ~ 2 pps ($= 1$ pps $\times 2$) based on the measured isomeric ratio [15]. The non-neutralized ^{198m,g}Tl$^+$ ions were extracted from the KISS gas cell with a probability of $\sim 10^{-4}$.

Figure 6(b) shows β-detection growth and decay curves associated with ^{198g}Os using $M = 2$ events in the MSPGC. For the first time, the half-life of ^{198g}Os was evaluated to be $T_{1/2} = 125(28)$ s (reduced $\chi^2 = 1.02$) by using Eqs. (3) and (4) for the β decay of the parent nucleus ^{198g}Os and the daughter nucleus ^{198g}Ir, respectively. Both functions expressed by Eqs. (3) and (4) for the internal decay of ^{198m}Tl and the β decay of ^{198g}Tl (both subsequent to internal decay of ^{198m}Tl and directly implanted) were used simultaneously in the time spectrum analysis. The function of Eq. (4) for ^{198g}Hg, the daughter nucleus of ^{198g}Tl, was not included because ^{198g}Hg is stable nucleus. The evaluated implantation rate of ^{198m}Tl (1 pps) and the estimated implantation rate of ^{198g}Tl (2 pps) were used in the analysis. However, these had negligible impact on evaluating half-life of ^{198g}Os due to much longer half-lives of ^{198m,g}Tl as compared to that of ^{198g}Os. Even though there might be some possibilities for other contaminant nuclei, with $A/q = 198$ and $Z > 77$, whose half-lives previously reported

(a)

Gated on 282.7 keV (^{198m}Tl)

(b)

—— Total	—·—·— ^{198g}Os	—·— ^{198m}Tl
— — BG	······ ^{198g}Ir	—··—·· ^{198g}Tl

(c)

Gated on 230.6 keV (^{198g}Os)
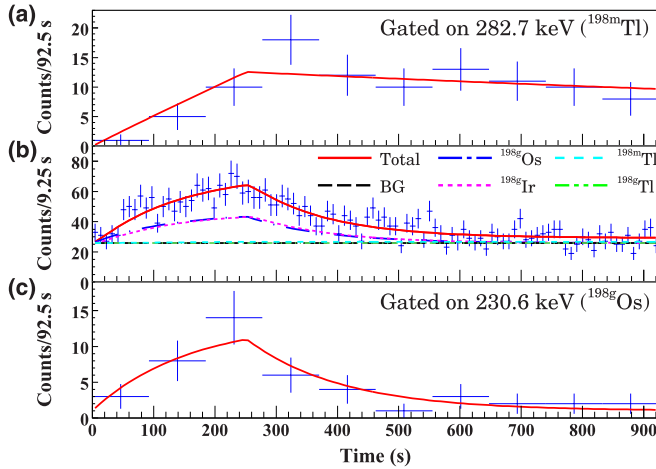
Time (s)

FIG. 6. Measured time spectra with the time sequence of $T_{on}/T_{off} = 252/672$ s. Here, the experimental particle-selection condition was osmium ($Z = 76$) selection by laser resonance ionization and $A/q = 198$ selection. (a) the growth and decay curves obtained by gating on the 282.7-keV γ ray emitted from the contaminant nucleus ^{198m}Tl. Here, $T_{1/2}$ and amplitude are free parameters. (b) time spectra of β rays detected by the MSPGC ($M = 2$). Solid line (red) is the best-fit curve, which consists of the constant background [long-dashed (black) line, free parameter] and four growth and decay curves as follows: dash-dotted (blue) line for ^{198g}Os ($T_{1/2}$ and the implantation rate are free parameters), dotted (purple) line for the daughter nucleus ^{198g}Ir (fixed $T_{1/2} = 8$ s [21] and amplitude was restricted by the implantation rate of ^{198g}Os), dashed (cyan) and double-dotted-dashed (green) lines for the contaminant nuclei ^{198m}Tl and ^{198g}Tl, respectively. In the analysis, $T_{1/2} = 1.87$ h and 5.3 h [21] of ^{198m}Tl and ^{198g}Tl, respectively, were fixed. The amplitudes were restricted by the evaluated implantation rates of ^{198m,198g}Tl. The line of ^{198g}Tl included two components stemmed from the ^{198g}Tl populated by the internal decay of ^{198m}Tl and the directly implanted ^{198g}Tl. (c) The growth and decay curves obtained by gating on the 230.8-keV γ ray emitted from ^{198g}Os as β-delayed γ ray. Here, $T_{1/2}$ and amplitude are free parameters.

[21] are much longer as compared to that of ^{198g}Os, they were not identified in the present measurements.

As listed in Table II, we observed the 64.9 keV and 73.6 keV characteristic x rays of iridium, the decay daughter of osmium. The half-lives obtained from gating on these x rays were comparable with our measured half-life of ^{198g}Os. The half-lives obtained by gating on the 407.22 keV and 507.3 keV γ rays in Table II were also consistent with the half-life of ^{198g}Os. This suggests that these γ rays were emitted from the β decay of the daughter nucleus ^{198g}Ir populated by the β decay of the parent nucleus ^{198g}Os. Because the half-life of ^{198g}Ir is much shorter than that of ^{198g}Os, the half-lives deduced by gating on these γ rays should be the same as that of ^{198g}Os. The evaluated γ-ray intensities per β decay of the daughter nucleus ^{198g}Ir from Fig. 5(b) were 10(4)% and 12(5)% for the 407.22 and 507.3-keV γ rays, respectively, and were consistent with those measured in the β decay of laser-ionized ^{198}Ir$^+$. These results strongly support the present measured β-decay half-life $T_{1/2} = 125(28)$ s of ^{198g}Os.

Figure 6(c) shows the time spectrum measured in coincidence with the 230.6-keV γ ray. The half-life of 108(36) s evaluated from Fig. 6(b) indicates that the 230.6-keV γ ray is the β-delayed γ ray of ^{198g}Os, which is emitted from an excited state of ^{198}Ir.

IV. DISCUSSION

A. ^{197}Os

A similar structure of a weakly deformed oblate shape between $^{197-199}$Os and $^{199-201}$Pt isotones was predicted from theoretical calculations [23,24]. From this similar structure in the isotone of ^{199}Pt [25], $I^{\pi} = 3/2^- (\nu(3p_{3/2}))$ or $5/2^- (\nu(2f_{5/2}))$ for ^{197g}Os is expected from the systematics of the neutron orbit and the similarity to ^{199}Pt levels [21,25]. In the present spectroscopic work, the I^{π} value was not identified. For the firm I^{π} assignment of ^{197g}Os, we will perform precise hyperfine structure measurement of ^{197g}Os by in-gas-jet laser ionization spectroscopy [26,27] as part of a future plan.

From the similarity to ^{199}Pt levels [21,25], a long-lived isomeric state with $I^{\pi} = 13/2^+$, which internally decays to ^{197g}Os, would exist in ^{197}Os. The long-lived isomer ^{197m}Os would be produced with about half of the intensity of ^{197g}Os by accounting for the present experimental results for the extraction of isomeric states of ^{197m,198m}Tl and ^{199m}Pt [15] produced by the MNT reactions. If the half-life of ^{197m}Os were sufficiently longer than 0.1 s for extraction from the KISS gas cell [12], we could identify it similar to the long-lived isomers ^{197m}Tl [$T_{1/2} = 0.54(1)$ s] and ^{198m}Tl [$T_{1/2} = 1.87(3)$ h] by measuring γ rays of internal transitions. However, we did not measure any unknown intense γ rays in the present measurement. This indicates that the half-life of ^{197m}Os might be much shorter than 0.1 s.

It was difficult to establish the complete β-decay scheme of ^{197g}Os from γ-γ coincidences because of the poor statistics. However, some of the γ-ray energies were in good agreement with the reported level energies of the excited states with I^{π} [28], which were identified by the ^{198}Pt($\vec{t}, \alpha$)^{197}Ir reaction. The states which show agreement in level energies are listed in Table I along with $\log(ft)$ values; here, the direct β transitions with the evaluated I_{γ} were assumed for the evaluation of the $\log(ft)$ values. Then, the β-transition strength to the ground state was evaluated to be $\geqslant 66(3)\%$ with the $\log(ft) \leqslant 5.93(4)$ from $1 - \Sigma I_{\gamma}$, by assuming direct β transitions with I_{γ} values listed in Table I. This would be an underestimation of the β-decay branching ratio to the ground state. However, the $\log(ft)$ values suggest that the direct β transitions to these states with $I^{\pi} = 1/2^+$, $3/2^+$, and $5/2^+$ are the FF transitions. This result also supports $I^{\pi} = 3/2^- (\nu(3p_{3/2}))$ or $5/2^- (\nu(2f_{5/2}))$ for ^{197g}Os.

B. ^{198}Os

The γ-ray intensity per β decay of ^{198g}Os was determined to be 20(6)% for the 230.6-keV transition in the present measurement. The β-decay branching ratios to ^{198g}Ir and the excited states of ^{198}Ir were tentatively evaluated to be $\leqslant 80(6)\%$ and $\leqslant 20(6)\%$ with $\log(ft) \geqslant 5.29(10)$ and $\log(ft) \geqslant 5.69(16)$, respectively, as shown in Fig. 7. We are now able to discuss
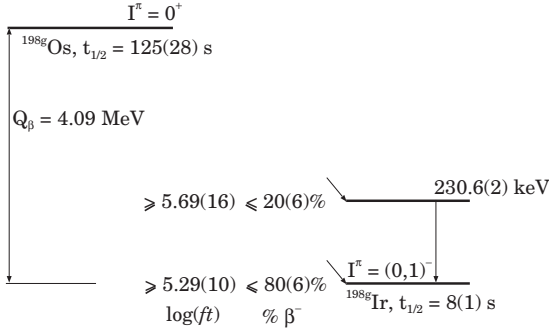
FIG. 7. Decay scheme of ^{198g}Os. The half-life of ^{198g}Os, β-decay intensities and the related $\log(ft)$ values, and γ-transition energies and intensities were newly measured. Spin-parity values and Q_β were the previously reported values [21].

FIG. 8. Measured β-decay half-lives (the present and previous results are marked by closed circles and squares, respectively) of osmium isotopes in comparison with the theoretical values of DF3 (open circles), FRDM (open squares), and KUTY (open triangles) models.

the structure of ^{198g}Ir from the present work, even though the poor statistics makes it difficult to establish complete β-decay schemes of ^{198g}Ir and ^{198g}Os from the measured γ-ray energy spectra. The intense β transitions of ^{198g}Os $\rightarrow$ ^{198g}Ir $\rightarrow$ ^{198g}Pt were observed as shown in Figs. 4 and 7 by accounting for the measured γ-ray intensities. From the analogy of ^{196g}Os β-decay chains [20] reported as FF transitions with small $\log(ft) \simeq 5.3$, $I^\pi = 0^-$ or 1^- for ^{198g}Ir was suggested. Considering the $I^\pi = 3/2^+$ $[\pi(2d_{3/2})]$ of heavier odd-A and the I^π systematics of even-A Ir isotopes [29], the wave functions of $I^\pi = 0^-$ or 1^- for ^{198g}Ir were expected to be $(\pi(2d_{3/2})) \otimes (\nu(3p_{3/2}))$ or $(\pi(2d_{3/2})) \otimes (\nu(2f_{5/2}))$, respectively.

C. Half-lives of Os isotopes

Generally, the FF transition for nuclei in the regions of $74 \leqslant Z \leqslant 82$ and $120 \leqslant N \leqslant 126$ [30] plays an important role in shortening the half-lives. Therefore, an appropriate treatment of the β-decay strength functions of these nuclei is required for theoretical predictions. For ^{197g}Os and ^{198g}Os, the FF transitions of $\nu(3p_{3/2})$ or $\nu(2f_{5/2}) \rightarrow \pi(2d_{3/2})$ are expected to be dominant in Table I, the β-decay schemes and I^π suggestions deduced in Figs. 4 and 7. The present measured half-lives were compared with those previously measured [21] and calculated from theories as shown in Fig. 8. Here, the theoretical models were the generalized energy-density functional (DF) theory with continuum quasiparticle random-phase approximation (QRPA) [31], the so-called DF3+QRPA (hereafter DF3), finite-range droplet model (FRDM) with QRPA [4] (hereafter FRDM), and the gross theory [32] with the KTUY mass model [5] (hereafter KTUY). These models include the allowed GT and FF transitions. The present measured half-lives are in good agreement with those calculated by using the KTUY model; the calculated values using DF3 and FRDM models overestimate and underestimate, respectively, the FF transitions of $\nu(3p_{3/2})$ and $\nu(2f_{5/2}) \rightarrow \pi(2d_{3/2})$. All the models reproduce the mea-

sured half-lives of the osmium isotopes partially in some mass range, but not over the entire mass range. This indicates that it is difficult to evaluate β-decay strength functions correctly, specifically, the FF transitions and its competition with GT transitions. The importance of precise experimental nuclear structure studies in this region around $N = 126$ in improving theoretical predictions is strongly suggested from the present results.
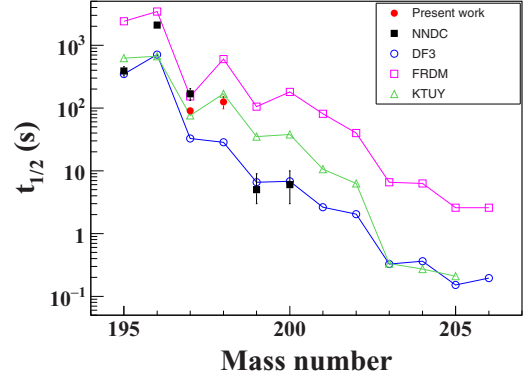
V. SUMMARY

For the purpose of astrophysical and nuclear structure studies, we performed β and γ spectroscopy of ^{197,198}Os and ^{198g}Ir, which were produced in the MNT reactions at KISS. The half-life of ^{197g}Os was revised to 91(8) s, while the half-life of ^{198g}Os has been measured for the first time and found to be $T_{1/2} = 125(28)$ s. The β-decay schemes of ^{198g}Ir and ^{198g}Os, including the suggested I^π for ^{198g}Ir, was partially established from the present spectroscopic work. From the present suggested I^π values of ^{197g}Os and ^{198g}Ir, the FF transitions of $\nu(3p_{3/2})$ or $\nu(2f_{5/2}) \rightarrow \pi(2d_{3/2})$ are suggested to be the dominant transitions. The present theoretical models reproduced the measured half-lives of osmium isotopes partially. The experimental study of nuclear structure in this region around $N = 126$ is important to improve theoretical predictions.

[1] E. M. Burbidge, G. R. Burbidge, W. A. Fowler, and F. Hoyle, Rev. Mod. Phys. **29**, 547 (1957).

[2] M. R. Mumpower, R. Surman, G. C. McLaughlin, and A. Aprahamian, Prog. Part. Nucl. Phys. **86**, 86 (2016).

[3] I. N. Borzov, Phys. Rev. C **67**, 025802 (2003).

[4] P. Möller, B. Pfeiffer, and K.-L. Kratz, Phys. Rev. C **67**, 055802 (2003).

[5] H. Koura, T. Tachibana, M. Uno, and M. Yamada, Prog. Theor. Phys. **113**, 305 (2005).

[6] G. Benzoni *et al.*, Phys. Lett. B **715**, 293 (2012).

[7] T. Kurtukian-Nieto *et al.*, Euro. Phys. J. A **50**, 135 (2014).

[8] A. I. Morales *et al.*, Phys. Rev. Lett. **113**, 022702 (2014).

[9] Y. Xu *et al.*, J. Radioanal. Nucl. Chem. **258**, 439 (2003).

[10] Y. Hirayama, Y. X. Watanabe, N. Imai, H. Ishiyama, S. C. Jeong, H. Miyatake, M. Oyaizu, S. Kimura, M. Mukai, Y. H. Kim, T. Sonoda, M. Wada, M. Huyse, Y. Kudryavtsev, and P. V. Duppen, Nucl. Instrum. Methods Phys. Res. B **353**, 4 (2015).

[11] Y. Hirayama, Y. X. Watanabe, N. Imai, H. Ishiyama, S. C. Jeong, H. S. Jung, H. Miyatake, M. Oyaizu, S. Kimura, M. Mukai, Y. H. Kim, T. Sonoda, M. Wada, M. Huyse, Y. Kudryavtsev, and P. V. Duppen, Nucl. Instrum. Methods Phys. Res. B **376**, 52 (2016).

[12] Y. Hirayama, Y. X. Watanabe, M. Mukai, M. Oyaizu, M. Ahmed, H. Ishiyama, S. C. Jeong, Y. Kakiguchi, S. Kimura, J. Y. Moon, J. H. Park, P. Schury, M. Wada, and H. Miyatake, Nucl. Instrum. Methods Phys. Res. B **412**, 11 (2017).

[13] Y. X. Watanabe, Y. H. Kim, S. C. Jeong, Y. Hirayama, N. Imai, H. Ishiyama, H. S. Jung, H. Miyatake, S. Choi, J. S. Song, E. Clement, G. de France, A. Navin, M. Rejmund, C. Schmitt, G. Pollarolo, L. Corradi, E. Fioretto, D. Montanari, M. Niikura, D. Suzuki, H. Nishibata, and J. Takatsu, Phys. Rev. Lett. **115**, 172503 (2015).

[14] Y. Hirayama, M. Mukai, Y. X. Watanabe, M. Oyaizu, M. Ahmed, Y. Kakiguchi, S. Kimura, H. Miyatake, P. Schury, M. Wada, and S. C. Jeong, J. Phys. B **50**, 215203 (2017).

[15] Y. Hirayama, M. Mukai, Y. X. Watanabe, M. Ahmed, S. C. Jeong, H. S. Jung, Y. Kakiguchi, S. Kanaya, S. Kimura, J. Y. Moon, T. Nakatsukasa, M. Oyaizu, J. H. Park, P. Schury, A. Taniguchi, M. Wada, K. Washiyama, H. Watanabe, and H. Miyatake, Phys. Rev. C **96**, 014307 (2017).

[16] M. Mukai *et al.* (unpublished).

[17] A. Winther, Nucl. Phys. A **572**, 191 (1994).

[18] A. Winther, Nucl. Phys. A **594**, 203 (1995).

[19] M. Mukai, Y. Hirayama, Y. X. Watanabe, P. Schury, H. S. Jung, M. Ahmed, H. Haba, H. Ishiyama, S. C. Jeong, Y. Kakiguchi, S. Kimura, J. Y. Moon, M. Oyaizu, A. Ozawa, J. H. Park, H. Ueno, M. Wada, and H. Miyatake, Nucl. Instrum. Methods Phys. Res. A **884**, 1 (2018).

[20] P. E. Haustein, E.-M. Franz, R. F. Petry, and J. C. Hill, Phys. Rev. C **16**, 1559 (1977).

[21] https://www.nndc.bnl.gov/.

[22] H. Xiaolong and Z. Chunmei, Nucl. Data Sheets **104**, 283 (2005).

[23] P. Möller, J. R. Nix, W. D. Myers, and W. J. Swiatecki, At. Data Nucl. Data Tables **59**, 185 (1995).

[24] L. M. Robledo *et al.*, J. Phys. G **36**, 115104 (2009).

[25] S. J. Steer *et al.*, Phys. Rev. C **84**, 044313 (2011).

[26] Y. Kudryavtsev, R. Ferrer, M. Huyse, P. V. den Bergh, and P. V. Duppen, Nucl. Instrum. Methods Phys. Res. B **297**, 7 (2013).

[27] R. Ferrer *et al.*, Nat. Commun. **8**, 14520 (2017).

[28] J. A. Cizewski, D. G. Burke, E. R. Flynn, Ronald E. Brown, and J. W. Sunier, Phys. Rev. C **27**, 1040 (1983).

[29] D. Verney *et al.*, Euro. Phys. J. A **30**, 489 (2006).

[30] H. Koura and S. Chiba, Phys. Rev. C **95**, 064304 (2017).

[31] I. N. Borzov, Phys. At. Nucl. **74**, 1435 (2011).

[32] T. Tachibana and M. Yamada, *Proceedings of the International Conference on Exotic Nuclei and Atomic Masses, ENAM95* (Editions Frontieres, Gif-sur-Yvette, 1995), p. 763, and references therein.